Experiments of Super-Resolution Utilizing Sub-Pixel Shifted Overlapping Images

Haruhisa SHIMODA and Kiyonari FUKUE
Tokai University Research and Information Center
2-28-4 Tomigaya, Shibuya-ku, Tokyo 151-0063, Japan
smd@keyaki.cc.u-tokai.ac.jp, fku@keyaki.cc.u-tokai.ac.jp

Abstract: Experiments for superresolution image reconstruction from subpixel shifted overlapping images has been performed for computer simulated image data in order to evaluate the primitive superresolution image reconstruction methods. The methods based on simultaneous equation showed comparatively small rms error according to the numerical solution. However, a high-resolution image was not obtained at ill-conditioned. The method based on local iteration showed good performance from view point of rms error and robustness.
Keywords: superresolution image reconstruction, multiframe-based superresolution, subpixel shifted overlapping images

1. Introduction

Superresolution is techniques to increases the spatial cutoff frequency of imaging system. It is known that software techniques of superresolution can be divided into two categories. The first is based on extrapolation of higher spatial frequency spectrum for a single low resolution image. The second is based on reconstruction of a high resolution image from subpixel shifted and overlapping low resolution multiple images. Approaches in the later category is called superresolution image reconstruction[1],[2] and multiframe-based superresolution [3], and etc.

Fundamental process of superresolution image reconstruction is image formation process from the desired high-resolution image as a target object to observed low-resolution images. The simplest linear image formation process can be express as:

$$\mathbf{Y}=\mathbf{WX} \qquad (1)$$

where vector **Y** is a low-resolution image, vector **X** is a high-resolution image, and matrix **W** is image formation matrix. The aim of the super-resolution reconstruction is to estimate **X** from **Y**. In this report, two kinds of primitive estimation method based on Eq.(1) are examined, that is, 1) the method based on the numerical solution of **X** and 2) the method based on local iteration of **Y**. The behavior and performance of these superresolution image reconstruction methods has been tested experimentally in this study.

2. Superresolution Image Reconstruction Method

(1) Model for Image Formation Process

Denote a low-resolution image of size N*M and a high-resolution image of size mN*mM by c(x,y) and f(x,y), respectively, where "m" is a magnification factor. Let consider Eq.(2) as a shift-invariant linear imaging model for c(x,y).

$$c_S(x,y)=\iint h(x+S-u,\, y+S-v)f(u,v)\,du\,dv \qquad (2)$$

where, h(u,v) is the point spread function(PSF) of the imaging system, and "s" is shift quantity for x and y direction. We assume the square point spread function as h(u,v).

$$h(u,v)=\begin{cases} 1/p^2, & \text{if } |u|\le p/2 \text{ and } |v|\le p/2 \\ 0, & \text{otherwise} \end{cases} \qquad (3)$$

This assumption is similar for the imaging system using CCD.

(2) Image Reconstruction Method Based on Simultaneous Equation

Figure 1 illustrates that the point spread function of a low-resolution pixel is overlaid on a high-resolution image, where a_{ij} is the area of the intersection of the high resolution pixel-j and low resolution pixel-i. In this case, the pixel value c_i of the low-resolution pixel-i is observed as follows:

$$c_i = \frac{1}{\sum_j a_{ij}} \sum_j a_{ij} f_j \quad , i=1,2,...,N_c \qquad (4)$$

where f_j is a pixel value of the high-resolution pixel-j. The normalizing term $\sum_j a_{ij}$ is 1.0 when area is measured with unit of a low-resolution pixel.

Eq.(4) can be obtained for the number N_c of observed low-resolution pixels. Thus, when N_c is greater than the number N_f of high-resolution pixels, pixel values of a high-resolution image can be obtained by solving the next simultaneous equation using least squares method[4].

$$\mathbf{C}=\mathbf{AF} \qquad (5)$$

where

$$\mathbf{C} = [c_1 \quad c_2 \quad \cdots \quad c_{N_c}]$$

$$\mathbf{F} = [f_1 \quad f_2 \quad \cdots \quad f_{N_f}]$$

$$\mathbf{A} = \begin{bmatrix} a_{11} & a_{12} & \cdots & a_{1N_f} \\ a_{21} & a_{22} & \cdots & a_{2N_f} \\ \vdots & \vdots & \ddots & \vdots \\ a_{N_c1} & a_{N_c2} & \cdots & a_{N_cN_f} \end{bmatrix}$$

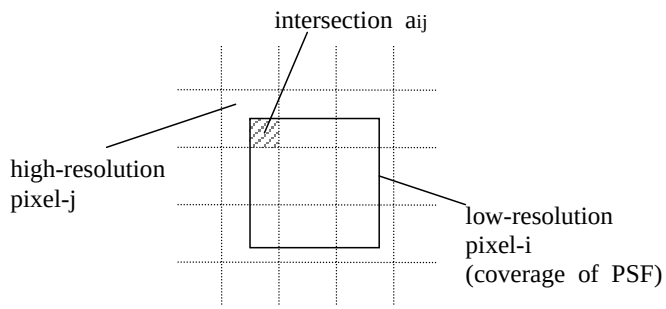

Figure 1. Relationship between a low-resolution pixel and high-resolution pixels.

(3) Image Reconstruction Method Based on Local Iteration

Irani,et.al.[5] proposed the following iterative reconstruction method. Starting with an arbitrary initial guess $f^{(0)}$ for the high-resolution image, the imaging process is simulated to obtain a set of low-resolution images $\{c_S^{(0)}\}$ corresponding to the observed input images $\{c_S\}$. If $f^{(0)}$ was the correct high-resolution image, then the simulated images $\{c_S^{(0)}\}$ should be identical to the observed images $\{c_S\}$. The each pixel value residual $\delta R^{(0)}(x,y)$ $(=c_S(x,y)-c_S^{(0)}(x,y))$ are then computed, and are distributed to the each pixel in the field of $f^{(0)}$ covered by PSF. This process is repeated iteratively to minimize the rms residual ΔR;

$$\Delta R^{(t)} = \sqrt{\frac{1}{\sum_S N_{c,S}} \sum_S \sum_{(x,y)} \left\{c_S(x,y) - c_S^{(t)}(x,y)\right\}^2} \qquad (6)$$

where $N_{c,s}$ is the number of pixels in $\{c_S\}$. Figure 2 shows this iterative process.

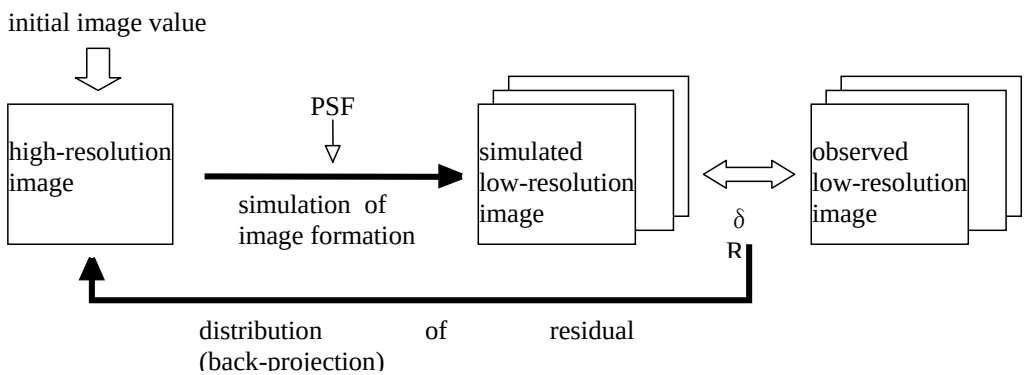

Figure 2. Schematic diagram of the iterative super-resolution reconstruction method.

When the square point spread function (Eq.(3)) is assumed as the PSF, a high-resolution pixel is updated by;

$$f^{(t+1)}(u,v)=f^{(t)}(u,v)+k\frac{1}{\sum_{(x,y)}\frac{a_{(u,v)\cap(x,y)}}{A_f}}\sum_{(x,y)}\left\{\frac{a_{(u,v)\cap(x,y)}}{A_f}\frac{a_{(u,v)\cap(x,y)}}{A_c}\delta R^{(t)}(x,y)\right\}$$

$$=f^{(t)}(u,v)+\frac{k}{\sum_{(x,y)}a_{(u,v)\cap(x,y)}}\sum_{(x,y)}\left\{a^2{}_{(u,v)\cap(x,y)}\delta R^{(t)}(x,y)\right\} \qquad (7)$$

where $a_{(u,v)\cap(x,y)}$ is an area that the high-resolution pixel at (x,y) overlaps with the low-resolution pixel at (u,v). A_f and A_c are an area of a high-resolution pixel and a low-resolution pixel, respectively. If an area is measured with unit of low-resolution pixel, A_c=1.0. "k", named update coefficient, is used to control updating speed.

3. Experiments

(1) Test Images

In our experiments, low-resolution images and desired high resolution images were created by simulation based on the imaging model Eq.(2) and PSF model Eq.(3) from digitized aerial photograph in size of 1000 1000 pixels, named the original image. Those low-resolution images were used as target observed images for image reconstruction. And those high-resolution images were used as true high-resolution images that should be produced by image reconstruction process. By using the true high-resolution image, the rms error ΔE can be defined as;

$$\Delta E=\sqrt{\frac{1}{N_f}\{f(u,v)-f_{true}(u,v)\}^2}\,. \qquad (8)$$

Because the size of twelve pixels on the original image was applied as the size of PSF (p in Eq.(3)), low-resolution images have the size of 83*83 pixels (Figure 3). Five sets of overlapping low-resolution images were produced for the cases of shift quantity S=1/12, 2/12, 3/12, 4/12, and 6/12 pixel on the low-resolution images. Table 1 shows relationship between shift quantity and the number of images contained in each set of overlapping low-resolution image.

Table 1. The number of images contained in low-resolution images set.

	low-resolution image set				
shift quantity (S)	1/12	2/12	3/12	4/12	6/12
the number of images	12*12	6*6	4*4	3*3	2*2

(a)S=(0,0) **(b)S=(6/12,0)** **(c)S=(0,6/12)** **(d)S=(6/12,6/12)**

Figure 3. Examples of low-resolution image.

(2) Applying the Reconstruction Method Based on Simultaneous Equation

Numerical solution techniques for simultaneous equation can be divided into elimination (direct) method and iteration (relaxation) method in general. We used solution algorithms of Doolittle elimination method and Gauss-Seidel iteration method for each these two solution technique.

The matrix **A** in Eq.(5) has the size of $N_{c,S}$*N_f. When N_c=83*83, S=1/12 ($N_{c,S}$=992,016) and N_f=996*996

correspond to the case of m=12, total amount of matrix elements is about 984 giga-elements. Because it is not practically that a main memory of a computer stores those all elements, simultaneous equations were set up for each sub-image such as 16*16 pixels on the low-resolution images in our experiments.

The image reconstruction based on simultaneous equations was applied to all sets of low-resolution images in the case of magnification factor m=12/8,12/7,12/6,12/5,12/4,12,3,12/2, and 12/1. Fig. 10 and Fig. 11 are the rms error of reconstructed high-resolution images by utilizing Doolittle elimination method and Gauss-Seidel iteration method, respectively. When the Doolittle method was utilized, the solution of the simultaneous equation was obtained only for m=8, 7, and 5. Because simultaneous equations became ill-conditioned or the number of equations had decreased more than the number of unknowns, the solution was not obtained for other values of m. When the Gauss-Seidel iteration method was utilized, solutions of the simultaneous equations were obtained in many cases in the case of Doolittle elimination method.

As can be seen in Figure 4 and Figure 5, Doolittle elimination method showed about 5-10 rms error in many cases, while Gauss-Seidel iteration method showed about 10-15 rms error in many cases. However, the rms errors increased in both cases when the number of low resolution pixels per a high resolution pixel decreases. Figure 6 shows high-resolution images reconstructed by Doolittle elimination method and Gauss-Seidel iteration method.

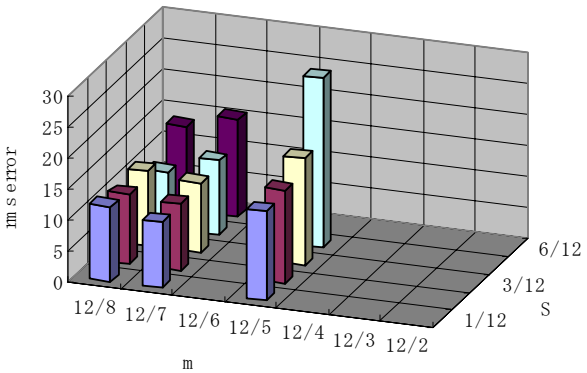

Figure 4. Rms error obtained by Doolittle elimination method.

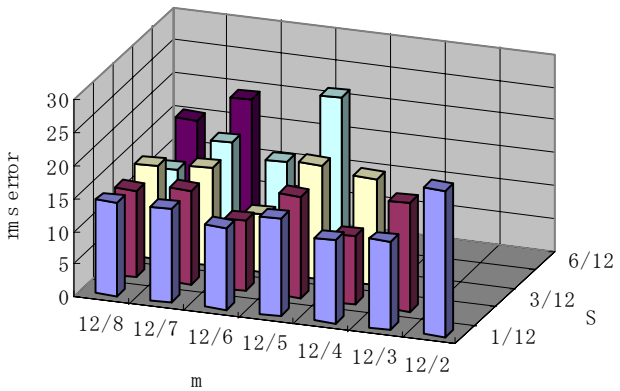

Fifure 5. Rms error obtained by Gauss-Seidel iteration method.

(1)m=12/5, S=1/12 (Doolittle elimination method) **(2)m=12/5, S=1/12 (Gauss-Seidel iteration method)** **(3)m=12/2, S=1/12 (Gauss-Seidel iteration method)**

Figure 6. Examples of reconstructed high-resolution image.

(3) Applying the Reconstruction Method Based on Local Iteration

The image reconstruction based on local iteration was applied to all sets of low-resolution images in the case of magnification factor m=12/8,12/7,12/6,12/5,12/4,12,3,12/2, and 12/1 as well as the reconstruction experiments based on simultaneous equation. A graph of the rms error/residual versus iteration number for the local iteration method is presented in Figure 7. The graph shows that rms error reaches a minimum then grows as the iteration

continues, while rms residual converges lower values. Furthermore, the graph shows that the iteration number at the minimum rms error increase as the update coefficient "k" increases. Figure 8 shows k-dependency for the minimum rms error and residual. As can be seen in Figure 8, it is clear that the minimum rms error depends on the update coefficient-k, and there is a optimal value of k because the minimum rms error hardly changes even if k is reduced too much that means increase the iteration number at the minimum rms error. Therefore, we used the optimal value of k in our reconstruction experiments.

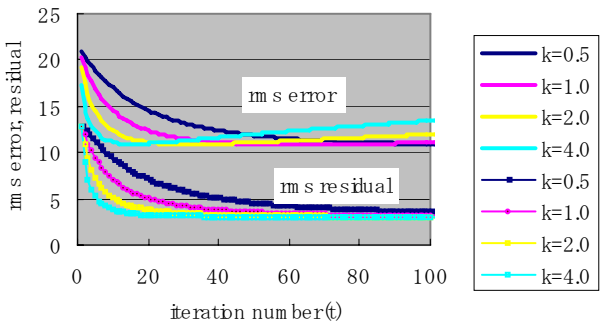

Figure 7. Rms error and rms residual versus iteration number.

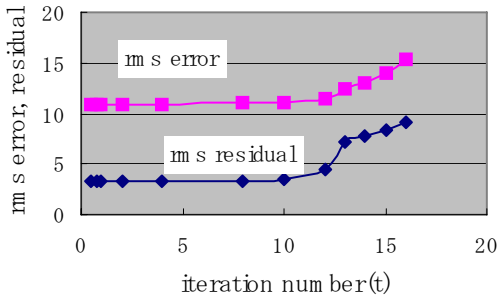

Figure 8. k-dependency of rms error and rms residual.

Figure 9 and Figure 10 show rms residual and rms error respectively. From Figure 9, we see that rms residual does not depend on shift quantity which corresponds to the number of utilizing low-resolution images. Furthermore, we see that rms residual increases when magnification factor-m decrease. Because rms residual is measured on low-resolution images, it seems the influence of aliasing.

Rms error were about 10 as shown in Figure 10, except when the number of low resolution pixels per a high resolution pixel was not small. These rms error are better than same values with compare to the case of Doolittle elimination method. Moreover, the iteration method produced the high-resolution images for all case of m and S unlike cases of the Doolittle elimination method. The high-resolution images reconstructed by local iteration method are shown in Figure 11.

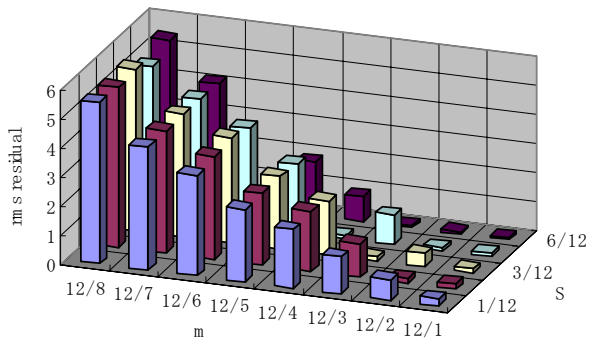

Figure 9. Rms residual obtained by the local iteration method.

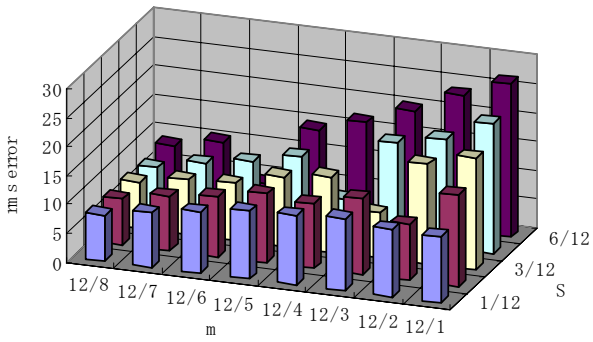

Figure 10. Rms error obtained by the local iteration method.

(a)m=12/5, S=1/12 (b)m=12/2, S=1/12 (c)m=12/1, S=1/12

Figure 11. Examples of high-resolution image reconstructed by local iteration method.

4. Conclusions

Image reconstruction experiments have been conducted by using primitive algorithms of superresolution image reconstruction based on simultaneous equation and local iteration. Doolittle elimination method and Gauss-Seidel iteration method were utilized for the reconstruction method based on simultaneous equation. Doolittle elimination method showed a smaller rms error than the Gauss-Seidel iteration method. But the case where the solution of the simultaneous equation was not obtained happened frequently for ill-conditioned cases compared with the Gauss-Seidel iteration method. Local iteration method showed the best performance from view point of rms error and robustness. However, rms error increased when the number of low resolution pixels per a high resolution pixel decreases. Furthermore, There is a problem in the setting of stop condition for the iteration because the behavior of the rms error（unknown for users） and the rms residual is different.

References

［1］ Sung Cheol Park, Min Kyu Park, and Moon Gi Kang, "Super-resolution image reconstruction: a technical overview," IEEE Signal Processing Magazine, p.21-36, May 2003.

［2］ Michel Elad and Arie Feuer, "Super-resolution reconstruction of image sequences", IEEE Trans. Pattern Analysis and Machine Intelligence, vol.21, no.9, pp.817-834, September 1999.

［3］ Fenghi Pan and Liming Zhang, "New image super-resolution scheme based on residual error restoration by neural networks," Optical Engineering, vol.42, no.10, pp.3038-30468, October 2003.

［4］ John Fryer and Kerry Mcintosh, "Enhancement of image resolution in digital photogrammetry," Photogrammetric Engineering & Remote Sensing, vol.67, no.6, pp.741-749, June 2001.

［5］ Michal Irani and Shmuel Peleg, "Improving resolution by image registration," CVGIP: Graphical Models and Image Processing, vol.53, no.3, May, pp.231-239, 1991.